ACS APPLIED MATERIALS & INTERFACES

Research Article

www.acsami.org

Fluorescent and Cross-linked Organic–Inorganic Hybrid Nanoshells for Monitoring Drug Delivery

Lijuan Sun,[†,#] Tianhui Liu,[‡,#] Hua Li,[§] Liang Yang,[§] Lingjie Meng,[*,‡] Qinghua Lu,[*,†] and Jiangang Long[§]

[†]School of Chemistry and Chemical Technology, State Key Laboratory of Metal Matrix Composites, Shanghai Jiaotong University, Shanghai 200240, P. R. China

[‡]School of Science, State Key Laboratory for Mechanical Behavior of Materials and [§]School of Life Science and Technology, Xi'an Jiaotong University, Xi'an 710049, P.R. China

Supporting Information

ABSTRACT: Functionalized and monodisperse nanoshells have attracted significant attention owing to their well-defined structure, unique properties, and wide range of potential applications. Here, the synthesis of cross-linked organic–inorganic hybrid nanoshells with strong fluorescence properties was reported via a facile precipitation polymerization of hexachlorocyclotriphosphazene (HCCP) and fluorescein on silica particles used as templates. The resulting poly(cyclotriphosphazene-*co*-fluorescein) (PCTPF) nanoshells were firm cross-linked shells with ~2.2 nm mesopores that facilitated the transport of drug molecules. The fluorescent nanoshells also exhibited excellent water dispersibility and biocompatibility; thus, they can be considered as ideal drug vehicles with high doxorubicin storage capacity (26.2 wt %) and excellent sustained release (up to 14 days). Compared to doxorubicin (DOX) alone, the PCTPF nanoshells more efficiently delivered DOX into and killed cancer cells. Moreover, the PCTPF nanoshells also exhibited remarkable fluorescent emission properties and improved photobleaching stability in both suspension and solid state owing to the covalent immobilization of fluorescein in the highly cross-linked organic–inorganic hybrids. The exceptional fluorescent properties enabled the release of DOX as well as the distribution of nanoshells and DOX to be monitored.

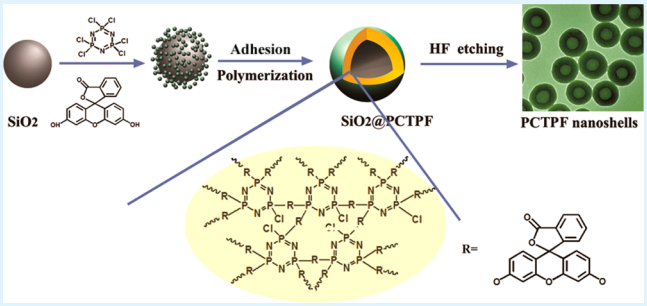

KEYWORDS: *poly(cyclotriphosphazene-co-fluorescein) (PCTPF), nanoshells, fluorescence, doxorubicin (DOX), drug delivery*

1. INTRODUCTION

Over the past few decades, monodisperse nanoshells have attracted significant attention owing to their well-defined structure, uniform size, and large surface area. These materials have found applications in diverse fields, such as drug delivery, catalysts, lithium-ion batteries, sensors, and so forth.[1−5] In the field of drug storage and release, nanoshells have advantages over conventional solid particles because of the simultaneous presence of a large cavity and penetrating mesoporous shells in their structure. The cavity and large surface area are beneficial for loading drug molecules, whereas the mesoporous shells afford accessible channels for the facile transport of drug molecules between the outer environment and inner void.

Nanoshells have been widely fabricated by a template-assisted process that involves coating templates with desired materials followed by selective removal of the templates by means of chemical etching or calcination. The templates can be either hard, such as silica,[6,7] polymer,[8,9] metal, and metal-oxide nanoparticles,[10,11] or soft, including micelles,[12,13] liquid drops,[14] and even gas bubbles.[15,16] However, a key issue resulting from many of these cases is that the nanoshells prepared by template-assisted methods are not compact or intact, leading to poor mechanical performance. A cross-linked shell can effectively tackle this problem; however, synthesis of organic cross-linkable shells is often a time-consuming, expensive, multistep process.[17−19]

Multifunctional nanoshells, synthesized by combining fluorescent, magnetic, and photothermal moieties onto the shells, are more interesting because of their obvious advantages in drug delivery and bioimaging.[20−22] However, the covering degree of functional moieties in most cases is low, and the distribution of functional moieties is also not uniform, inevitably leading to some drawbacks. For instance, fluorescent shells could be obtained by conjugating organic dyes, quantum dots, and other fluorophores on the nanoshells.[23,24] The quantum dots often encounter potential toxicity because of their heavy metal ingredients,[25] and the fluorescent dyes tend to not only aggregate or leak from the host systems but also suffer from an omnipresent concentration quenching effect.[26,27] Therefore, it is an ongoing challenge to prepare cross-linked, fluorescent nanoshells with favorable biocompatibility, excellent fluorescence properties, and high resistance to photobleaching.

Received: January 8, 2015
Accepted: February 5, 2015
Published: February 5, 2015

DOI: 10.1021/acsami.5b00175
ACS Appl. Mater. Interfaces 2015, 7, 4990−4997

Hexachlorocyclotriphosphazene (HCCP), a typical inorganic ring, is often used to synthesize cyclotriphosphazene-based materials. The resulting polyphosphazenes are versatile organic−inorganic hybrid polymers with organic groups attached to an inorganic backbone that consists of alternating single and double P−N bonds. On the basis of their excellent biocompatibility, tunable biodegradability, and unprecedented structural diversity, these hybrid polymers have been used to successfully coat other nanomaterials for biomedical applications.[28,29] The polyphosphazenes themselves could create some nanostructures, such as nanospheres,[30] nanotubes,[31,32] and so forth. Interestingly, we recently found that fluorescent dyes could exhibit high fluorescent efficiency at any concentration after being "fastened" and "isolated" into cross-linked polyphosphazene by covalent bonding.[33] Inspired by this finding, we realized that it might also be possible to fabricate various cross-linked polyphosphazene materials with significant fluorescence and biocompatibility by a facile reaction of proper fluorescent molecules with HCCP.

In this work, we developed a facile procedure for the preparation of new fluorescent, cross-linked organic−inorganic hybrid mesoporous nanoshells by growing poly(cyclotriphosphazene-*co*-fluorescein) (PCTPF) on silica nanospheres used as sacrificial templates. The structures and sizes of the PCTPF nanoshells could be aptly tuned by changing the molar ratio of monomers to silica particles. The pore size of the shells was ∼2.2 nm, which is big enough for transporting small drug molecules. As expected, the PCTPF nanoshells showed remarkable fluorescence and excellent photobleaching stability. It is noted that, compared to other well-developed synthetic procedures for preparing fluorescent, cross-linked hollow materials, our procedure is much more effective, facile, and repeatable. Realizing the advantages of these polyphosphazene materials, such as good biocompatibility, solvent resistance, and water dispersibility, we synthesized fluorescent, cross-linked PCTPF nanoshells. To the best of our knowledge, this is the first report on the application of fluorescent, cross-linked polyphosphazene nanoshells for visualizing the loading and controlled release of doxorubicin (DOX).

2. EXPERIMENTAL SECTION

2.1. Materials. Hexachlorocyclotriphosphazene (HCCP, 99%) and fluorescein (99%) were purchased from Adamas Reagent, Ltd. Anhydrous ethanol, ammonium hydroxide ($NH_3{\cdot}H_2O$), tetraethyl orthosilicate (TEOS), triethylamine (TEA), hydrofluoric acid (HF), and acetonitrile were obtained from Sinopharm Chemical Reagent Co., Ltd. The human cervical cell line HeLa was purchased from the Cell Resource Centre of Life Sciences. Bovine serum albumin (BSA, 66 kD, >98%), fetal bovine serum (FBS), and Dulbecco's modified Eagle medium (DMEM) were obtained from Gibco BRL. WST-8 reagent was purchased from Beyondtime Bio-Tech. Doxorubicin (DOX) hydrochloride and 4′,6-diamidino-2-phenylindole dihydrochloride (DAPI, 98%) were purchased from Shanghai Yingxuan Reagent Co., Ltd. and Sigma, respectively. All chemicals were used as received without any further purification. Water was purified using a Milli-Q-system (Millipore).

2.2. Synthesis of Silica Nanospheres. Silica nanospheres were prepared following a previously published procedure with slight modification.[34] In a typical experiment, tetraethyl orthosilicate (2 mL) was mixed with anhydrous ethanol (18 mL) to obtain a stock solution (termed solution A). Ammonium hydroxide (20 mL) was mixed with anhydrous ethanol (60 mL) to prepare solution B. Solution A (2 mL) was then added dropwise to solution B while stirring vigorously. The resulting mixture was rapidly stirred at room temperature until the solution became turbid. Suspended white colloidal particles were collected by centrifugation at 8000 rpm for 5 min, washed with ethanol (10 mL × 3), and finally dispersed in acetonitrile (50 mg/mL) as a stock solution.

2.3. Preparation of PCTPF Nanoshells. Silica (SiO_2) nanospheres were dispersed in acetonitrile (0.2 mg/mL, 50 mL) by ultrasonication. HCCP (20 mg), fluorescein (60 mg), and TEA (2 mL) were then added to the suspension. The mixture was subjected to ultrasonic irradiation (100 W, 40 kHz) for 6 h at room temperature. The resulting SiO_2@PCTPF were collected by centrifugation and washed with ethanol (10 mL × 3). For fluorescent nanoshells to be obtained from removal of the SiO_2 cores, an aqueous HF solution (10 mL, 1 M) was added to the solution and stirred for another 2 h. After etching, the fluorescent PCTPF shells were isolated by centrifugation, washed with deionized water and ethanol (10 mL × 3), respectively, and then dried under vacuum at 40 °C.

2.4. Drug Storage and Release. PCTPF shells (5 mg) were dispersed in phosphate buffer solution (5 mL PBS, pH 7.4) under ultrasonic irradiation (100 W, 40 kHz) for 30 min. DOX hydrochloride (2.5 mg) was then added, and the mixture was stirred for 24 h at room temperature in the dark to reach an equilibrium state. The DOX-loaded PCTPF shells (denoted as PCTPF-DOX) were collected by repeated ultracentrifugation with PBS until the supernatant was color free. The amount of unbound DOX was determined by measuring the absorbance at 480 nm relative to a calibration curve recorded under the same conditions. The mass of DOX loaded into PCTPF was calculated by subtracting the mass of DOX in the supernatant solution from the total mass of DOX. An in vitro drug release test was performed by immersing the PCTPF-DOX (1 mg) in pH 7.4 and 5.5 PBS buffered solutions (5 mL) under gentle stirring at 37 °C. At different time intervals, the sample was separated from the buffer by ultracentrifugation, and the concentration of released DOX in the supernatant was determined by measuring the UV absorbance at 480 nm.

2.5. Cell Viability Test. The biocompatibility of PCTPF nanoshells was quantitatively assessed by WST-8 assays.[35,36] HeLa cells were seeded into a 96-well flat culture plate (Corning) with 200 μL of DMEM (high glucose) supplemented with 10% FBS per well. They were cultured in a humidified incubator at 37 °C in which the CO_2 level was maintained at 5%. After incubating overnight to allow cell attachment, the HeLa cells were incubated with PCTPF nanoshells (10, 20, 50, and 100 μg/mL in FBS-free culture medium) at 37 °C for 24 and 48 h, respectively. Subsequently, 20 μL of the WST-8 reagent was added to the wells. After incubating the cells for another 2 h, the absorbance of the resulting solution mixture was measured at 450 nm by a microplate reader (Bio-Rad, model 680). Cells cultured without PCTPF nanoshells over the same time intervals were used as controls. Cell viability was calculated as the percentage of absorbance of the sample well compared to that of the control well containing untreated cells.

The cytotoxicity of DOX and PCTPF-DOX was evaluated with a modified procedure. The attached HeLa cells were incubated with PCTPF-DOX or DOX at different concentrations for 1 h, were washed with sterilized PBS, and were then incubated in fresh culture media (10% FBS) for another 5, 24, or 48 h. Cell viability was assessed by a WST-8 assay.

2.6. Cell Imaging. HeLa cells were seeded into a 12-well flat culture plate (Corning) and cultured in DMEM supplemented with 10% FBS, 100 units/mL penicillin, and 100 μg/mL streptomycin at 37 °C overnight. The cells were washed with FBS-free DMEM, incubated with PCTPF-DOX (50 μg/mL in FBS-free culture medium) at 37 °C for another 1h, and then washed with PBS and FBS-free DMEM to remove the free PCTPF-DOX. The fresh, FBS-free DMEM was used as a substitute for the culture medium to incubate for another 0, 3, and 5 h. The cells were fixed in paraformaldehyde (4 wt %) for 30 min, followed by washing with PBS (2 × 2 mL). The fixed cells were then stained in a DAPI solution (0.1 μg/mL) for 15 min, washed with PBS (2 × 2 mL), and observed under a confocal laser scanning microscope.

2.7. Characterization. Transmission electron microscopy (TEM) analysis was conducted with a JEOL JEM-2100 electron microscope operated at 200 kV. Field emission scanning electron microscope (FE-

DOI: 10.1021/acsami.5b00175
ACS Appl. Mater. Interfaces 2015, 7, 4990−4997

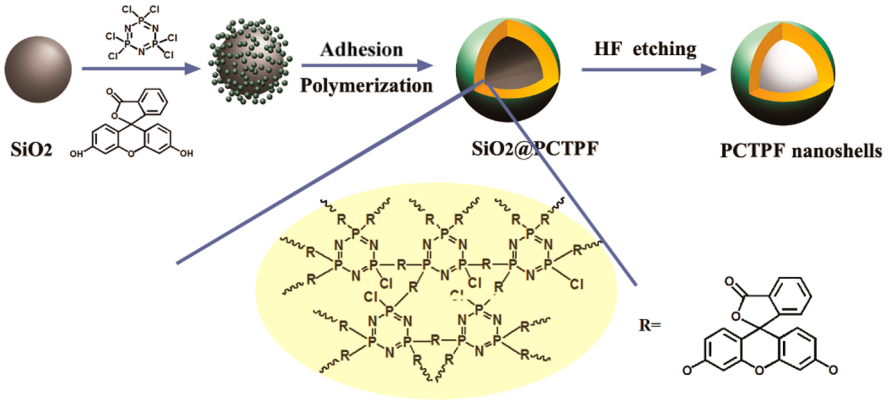

Figure 1. Scheme of the synthetic procedure for generating PCTPF nanoshells.

SEM) images were obtained using a Philips Sirion 200 instrument under an accelerating voltage of 20 kV. The size and distribution of all of the prepared nanomaterials were determined from TEM and SEM micrographs using ImageJ (V1.41, NIH) for image analysis. Dynamic light scattering (DLS) measurements were carried out on a zetasizer Nano ZS from Malvern Instruments with a laser at 633 nm. Photographs were taken with a digital camera (IXUS 800IS, Canon). Fourier-transform infrared (FTIR) spectra were recorded on a Paragon 1000 (PerkinElmer) spectrometer. Samples were dried overnight at 45 °C under vacuum and thoroughly mixed and crushed with KBr to fabricate KBr pellets. Nitrogen adsorption−desorption isotherms and pore size distributions were obtained on an ASAP 2010 M+C surface area and porosimetry analyzer after the samples were pretreated at 40 °C under vacuum for dehydration. Ultraviolet and visible (UV−vis) absorption spectra were recorded on an Shimadzu UV-2550 spectrophotometer. Fluorescence spectra were obtained using a Perkin−Elmer LS 50B fluorescence spectrometer. Fluorecence images of cells were taken on a LSM700 confocal laser scanning microscopy (Carl Zeiss, He−Ne and Ar lasers).

3. RESULTS AND DISCUSSION

The preparation of PCTPF nanoshells is a quite straightforward process based on one-pot synthesis of cross-linked PCTPF nanoshells on silica nanospheres followed by etching of the templates (Figure 1). Silica (SiO_2) templates were first prepared according to a modified procedure.[34] The polycondensation of HCCP with fluorescein was then conducted in an ultrasonic bath at room temperature in acetonitrile. The hydroxyl groups on the fluorescein were activated by TEA and tended to attack the nuclei of phosphorus atoms on HCCP. Excess TEA acted as an acid acceptor to absorb the resulting HCl and accelerate polymerization.[29,37] The resulting cross-linked PCTPF nanoparticles were formed and automatically diffused onto the surface of SiO_2 because of the low surface energy of PCTPF. The cross-linking reaction among the PCTPF nanoparticles was then carried out continuously, leading to the formation of shells on the surface of the SiO_2 nanospheres. Finally, the SiO_2 templates were directly etched by HF solution to obtain cross-linked PCTPF nanoshells.

The structures and morphologies of SiO_2 particles, SiO_2@PCTPF particles, and PCTPF nanoshells were investigated by TEM and SEM (Figure 2). The prepared SiO_2 particles with relatively smooth outer surfaces had an average diameter of 165 ± 15 nm (Figure 2a). After the silica templates were coated by PCTPF, the core@shell structure of SiO_2@PCTPF particles was clearly observed due to the electronic contrast of PCTPF shells to SiO_2 cores (Figure 2b). The SiO_2 cores in SiO_2@PCTPF particles were etched by HF to obtain PCTPF

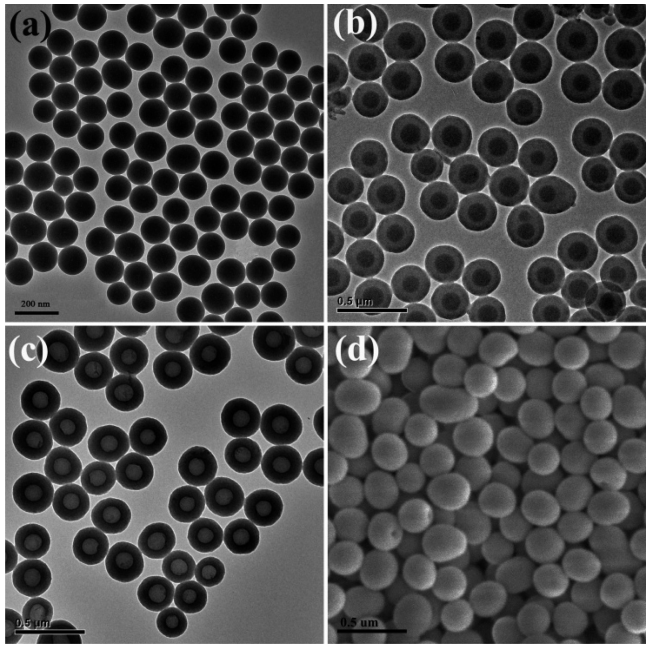

Figure 2. TEM images of (a) silica nanoparticles, (b) SiO_2@PCTPF particles, and (c) PCTPF nanoshells and (d) SEM image of PCTPF nanoshells.

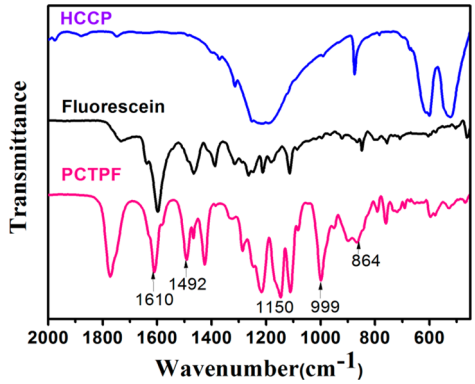

Figure 3. FTIR spectra of HCCP, fluorescein, and PCTPF nanoshells.

nanoshells. Figure 2c shows that in contrast to the TEM image of SiO_2@PCTPF particles, the TEM image of the PCTPF nanoshells has a high electron beam transmitted area, suggesting the formation of a hollow structure. The SEM image

DOI: 10.1021/acsami.5b00175
ACS Appl. Mater. Interfaces 2015, 7, 4990−4997

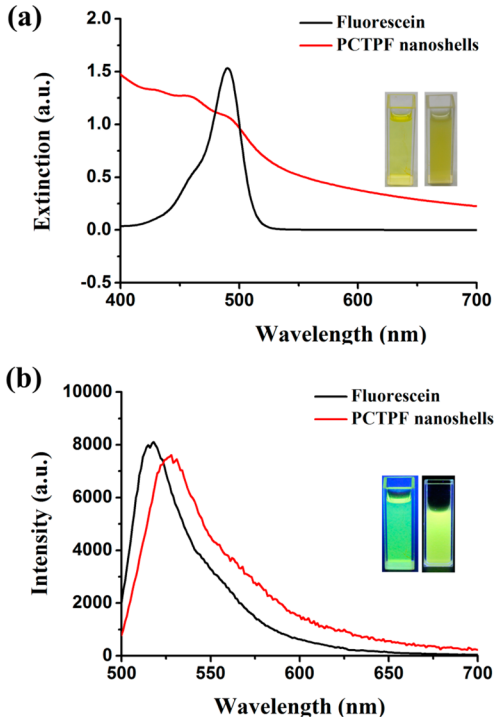

Figure 4. (a) UV−vis absorption spectra and (b) fluorescence emission spectra (λ_{ex} = 470 nm) of fluorescein and PCTPF nanoshells in ethanol. Inset images in (a) photographs and (b) fluorescence photographs (irradiating at 365 nm) of fluorescein (left) and PCTPF nanoshells (right) in ethanol.

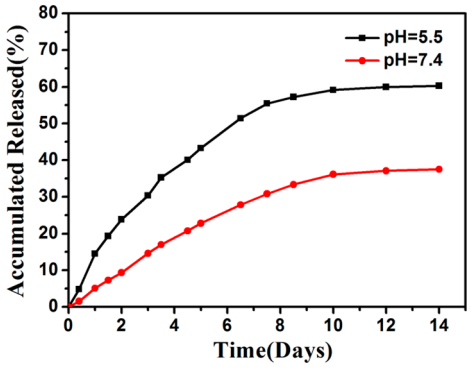

Figure 6. In vitro release behaviors of DOX from PCTPF-DOX nanoshells in PBS at different pH values at 37 °C.

further gave direct evidence that most of the nanoshells had complete spherical shells (Figure 1d). The average size of the SiO_2@PCTPF particles as well as PCTPF nanoshells was ∼265 nm as determined from Figure 2b and 2c. DLS measurements determined that the average diameter of the PCTPF nanoshells was 297 nm, a bit bigger than that observed from TEM; this is due to the hydrophilic nature of PCTPF (see Supporting Information, Figure S1). Thus, the average thickness of the PCTPF shells was ∼50 nm with interior cavities of ∼150 nm in diameter.

The size and structure of the synthesized PCTPF nanoshells were tuned by adjusting the mass ratio of SiO_2 and the precursors of PCTPF. To prepare a series of PCTPF nanoshells, we fixed the concentration of SiO_2 at 0.2 mg/mL while adjusting the mass of HCCP and fluorescein from 0.2 and 0.6 mg/mL, respectively, to 1 and 3 mg/mL, respectively (see Supporting Information, Figure S2). When HCCP and fluorescein were at relatively low concentrations (0.2 and 0.6 mg/mL, respectively), thin deformed PCTPF nanoshells were obtained. When the mass of HCCP and fluorescein were 0.4 and 1.2 mg/mL, respectively, well-defined nanoshells with a single regular cavity were fabricated. When the mass of HCCP and fluorescein were increased to 0.75 and 2.25 mg/mL, respectively, or higher, we obtained bigger nanoshells (>300 nm) with multicavity structures because the excess PCTPF might coat two or three SiO_2 nanoparticles together.

FTIR spectroscopy was used to characterize the chemical structure of the PCTPF nanoshells (Figure 3). The new intensive absorption at 999 cm^{-1} was attributed to the presence of P−O−Ar, confirming the polymerization of HCCP and fluorescein. We also observed other characteristic peaks of PCTPF, including at 1149 and 864 cm^{-1} (P═N) in the cyclotriphosphazene structure, and at 1610 and 1492 cm^{-1} (Ph), 1215 cm^{-1} (C−O−C), and 1112 cm^{-1} (Ar−H) in the fluorescein moieties.[38]

The fluorescence spectra of PCTPF nanoshells and fluorescein in ethanol were compared. Both fluorescein and PCTPF nanoshells in ethanol are yellow in color; they also show strong absorption at ∼490 nm, but the baseline of the ethanol dispersion of PCTPF nanoshells increased significantly due to the colloid nature of the nanoshells (Figure 4a). Therefore, we investigated the fluorescence properties of fluorescein and PCTPF nanoshells in ethanol using 470 nm as the excitation wavelength (λ_{ex}). The ethanol solution of fluorescein exhibited a strong emission peak at 517 nm, whereas the emission peak of the ethanol dispersion of PCTPF nanoshells was red-shifted to 526 nm (Figure 4b). The

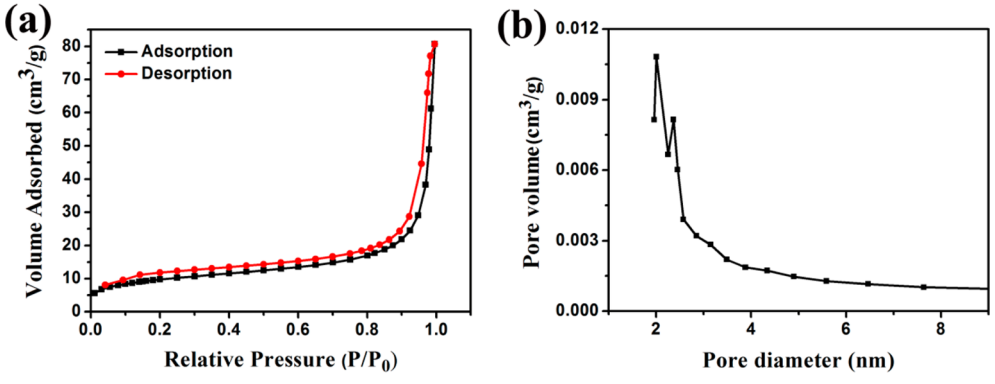

Figure 5. (a) Nitrogen adsorption−desorption isotherms and (b) pore size distribution of the PCTPF nanoshells.

DOI: 10.1021/acsami.5b00175
ACS Appl. Mater. Interfaces 2015, 7, 4990−4997

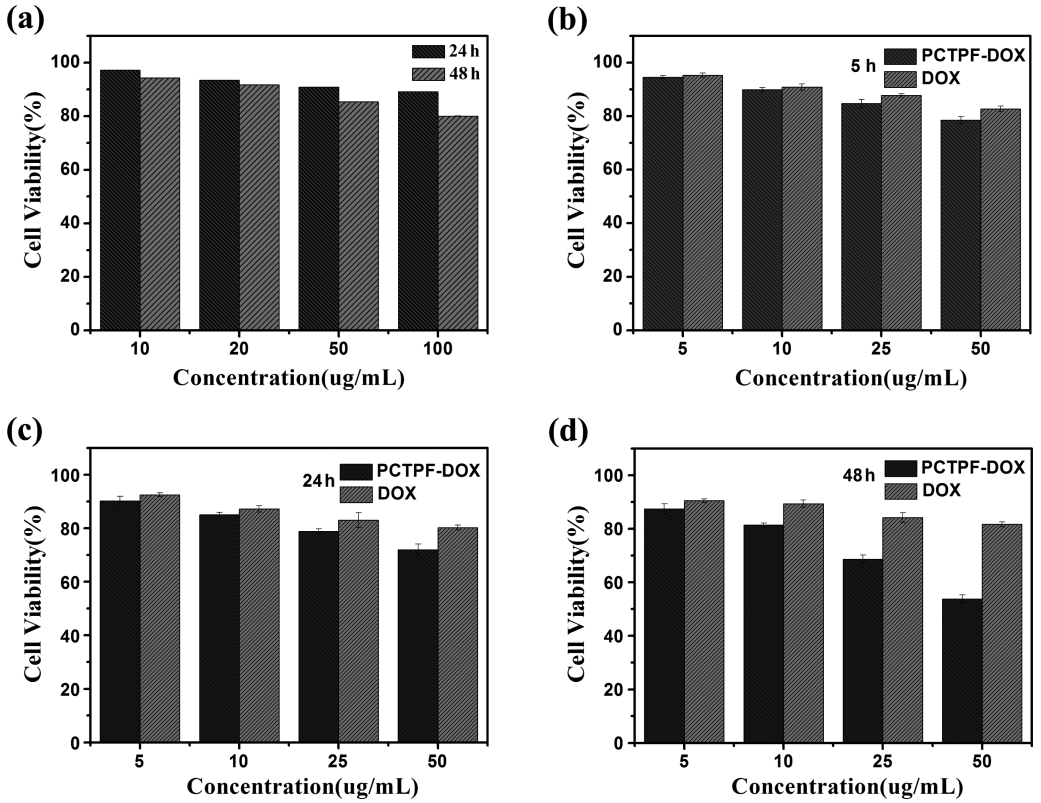

Figure 7. Viability of HeLa cells incubated with (a) PCTPF nanoshells at different concentrations for 24 and 48 h and (b–d) PCTPF-DOX and DOX at different concentrations for 1 h, washed with sterilized PBS, then incubated in fresh culture media (10% FBS) for another (b) 5, (c) 24, and (d) 48 h.

fluorescence photographs of fluorescein and PCTPF nanoshells in ethanol were green and yellow-green, respectively (inset, Figure 4b).

Interestingly, PCTPF nanoshells exhibited resistance to photobleaching that was superior to that of fluorescein and effectively overcame aggregation-induced quenching (see Supporting Information, Figure S3). Similar to other organic dyes, the fluorescence of the fluorescein solution gradually weakened under irradiation of 2 W of UV light, indicating photobleaching (see Supporting Information, Figure S3a). However, the fluorescence of the PCTPF nanoshell dispersion showed negligible quenching even after irradiating under 2 W of UV light for 150 min. This suggests that the fluorescein moieties achieve improved photochemical stability after being "fastened" in the cross-linked structures. In addition, the fluorescein solution exhibited very weak fluorescence at high concentration due to aggregation-induced quenching (e.g., the fluorescein powder is nonfluorescent). However, the PCTPF nanoshells exhibited remarkable fluorescent emission features at any concentration even in the solid state (see Supporting Information, Figure S4). The cyclotriphosphazene rings are nonconjugated systems for electron transfer and are photochemically inert because their backbone consists of alternating P–N single and double bonds without any resonance between them.[39] Therefore, the cyclotriphosphazene rings serve as spacers to isolate the fluorescein units on the nanoshells, effectively blocking electron transfer as well as energy transfer among the fluorescein units and thus reducing fluorescence quenching at any concentration.

The Brunauer–Emmett–Teller (BET) surface area and pore size of the PCTPF nanoshells were investigated by nitrogen adsorption experiments (Figure 5). The adsorption–desorption isotherms of the PCTPF nanoshells exhibited type IV isotherms with two distinct adsorption steps at relative pressures of 0.2–0.5 and 0.7–0.99 (Figure 5a). On the basis of the pore size distribution curves (Figure 5b), the first step should correspond to nitrogen capillary condensation in the mesopores (~2.2 nm) of the PCTPF nanoshells. The second adsorption step is mainly due to the inner cavities of the PCTPF nanoshells, as observed in TEM images. The BET surface area of the PCTPF nanoshells was calculated to be 34.2 m^2/g. The shells with mesopores and hollow central cavities might show advantages for applications such as drug loading and delivery.

We selected DOX, a typical anticancer drug, for evaluating the loading and release behaviors of PCTPF nanoshells as drug carriers. In the DOX loading process, the DOX molecules are entrapped within the hollow structure and mesochannels by an impregnation process. The PCTPF-DOX nanoshells were collected by centrifugation to remove the supernatant and dried under vacuum before being resuspending in aqueous solution. Up to 355 mg of DOX could be stored in 1 g of PCTPF nanoshells; therefore, the loading efficiency is ~26 ± 2 wt % at pH 7.4.

The in vitro release properties of DOX from PCTPF nanoshells in PBS buffer solutions at different pH values (pH 5.5 and 7.4) at 37 °C were studied (Figure 6). The release of PCTPF-DOX was found to be pH dependent. The release of DOX from the PCTPF nanoshells in a slightly acidic solution (pH 5.5, corresponding to lysosomal pH) was observed over a 14 day period and found to be accelerated compared to that in a neutral solution (pH 7.4, corresponding to blood pH). This

DOI: 10.1021/acsami.5b00175
ACS Appl. Mater. Interfaces 2015, 7, 4990–4997

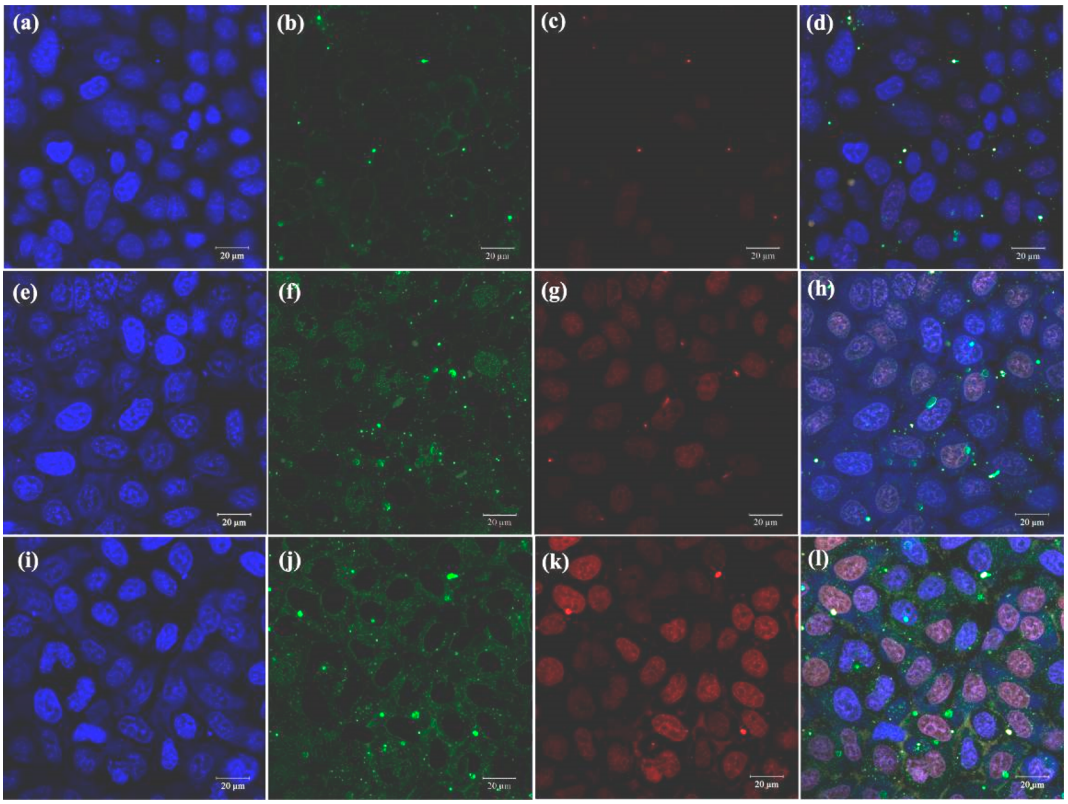

Figure 8. Representative fluorescence images of HeLa cells incubated with 50 μg/mL PCTPF-DOX for 1 h, washed with sterilized PBS, then incubated in fresh culture media (10% FBS) for another (a−d) 0 h, (e−h) 3 h, or (i−l) 5 h. The cells were then fixed in paraformaldehyde (4%) for 10 min and stained in a DAPI solution (0.1 μg/mL) for 20 min before being observed by confocal laser scanning microscopy under irradiation of (a, e, i) 360 nm, (b, f, j) 450 nm, and (c, g, k) 580 nm; d, h, and l are merged images.

pH-dependent drug release might result from a larger degree of protonation of the carboxyl and amino groups on DOX at lower pH,[40] weakening the interaction between DOX and the PCTPF nanoshells. The pH-dependent DOX release might greatly improve pharmaceutical efficiency and reduce side effects because DOX favors release in acidic microenvironments such as intracellular lysosomes and endosomes and cancerous tissues.

In several drug delivery systems, burst release often occurs over the first several hours; drug release may even be complete in 1 day.[41,42] In contrast, PCTPF-DOX exhibited excellent sustained release properties. Only 60% (pH 5.5) and 30% (pH 7.4) of the loaded DOX was released even after 8 days. Both the mesochannels and strong interactions between DOX and PCTPF effectively retarded the burst release of DOX molecules from the interior cavities.

For quantitative assessment of the cytotoxicity of PCTPF nanoshells, HeLa cells were assayed using a WST-8 assay kit. The HeLa cells incubated with PCTPF nanoshells did not result in severe cytotoxicity over a wide concentration range (10−100 μg/mL) for 24 or 48 h. Cell viability was higher than 80% for all cases, indicating low biological toxicity of PCTPF nanoshells (Figure 7a). Therefore, PCTPF nanoshells can safely be used for biological applications such as bioimaging and drug delivery.

The efficacy of PCTPF-DOX and DOX to kill cancer cells was also measured in HeLa cells by WST-8 assays. HeLa cells were treated with DOX at different concentrations (5−50 μg/mL) for 1 h and then cultured in fresh media for 5, 24, and 48 h. Their viability was higher than 75% for all concentrations (Figure 7b−c) probably because of the difficulty of DOX being able to enter the HeLa cells. However, over the same intervals, the viability of PCTPF-DOX treated cells exhibited a dramatic decline with prolonged culture time and increased drug concentration (Figure 7b−c). Thus, we postulated that PCTPF-DOX nanoshells preferred to enter the cells, and DOX was then released gradually from the mesopores and inner cavities. The therapeutic efficiency of PCTPF-DOX was obviously time- and dosage-dependent due to the nanoshells excellent sustained release properties. Therefore, the PCTPF nanoshells can be considered potential vehicles that might improve the delivery of anticancer drugs into cancer cells.

The location and distribution of nanoshells and DOX release in HeLa cells were investigated by fluorescence imaging with a confocal laser scanning microscope (Figure 8). After the cells were stained with DAPI, the nuclei of HeLa cells exhibited bright blue fluorescence while being irradiated with a 360 nm laser (Figure 8a, e, and i).[43,44] The PCTPF nanoshells and DOX emitted green and red fluorescence at λ_{ex} = 450 and 580 nm, respectively. However, PCTPF-DOX showed severe fluorescence quenching due to $\pi-\pi$ stacking interactions between DOX and the fluorescein moieties in PCTPF nanoshells. When the HeLa cells were incubated with PCTPF-DOX for only 1 h, they exhibited negligible fluorescence under irradiation at both 450 and 580 nm because little DOX was released from the PCTPF-DOX nanoshells (Figure 8b and c). With prolonged incubation time, more DOX was released, and consequently, the fluorescence intensity of both PCTPF and DOX was gradually enhanced (Figure 8f, g, j, and k). The fluorescent regions of PCTPF nanoshells are in

DOI: 10.1021/acsami.5b00175
ACS Appl. Mater. Interfaces 2015, 7, 4990−4997

good agreement with those of DOX. Upon the emissions images being merged, regions of yellow color can be seen inside the cells, which indicates that the PCTPF-DOX nanoshells have been internalized inside the cells and concentrated in the cytoplasm. In Figure 8j and k, the cells are almost fully stained by nanoshells and DOX, indicating efficient uptake of PCTPF-DOX into the HeLa cells in the first 1 h, and more DOX release after 5 h. Thus, the above findings suggest that the PCTPF nanoshells not only successfully cross intracellular membranes and deliver drugs into cells, but they also provide a subtle mechanism for monitoring drug delivery and release due to the fluorescent nature of the nanoshells.

4. CONCLUSIONS

In summary, we developed a facile but effective method to fabricate fluorescent and cross-linked nanoshells via precipitation polymerization of fluorescein and hexachlorocyclotriphosphazene using silica particles as a template. The morphology and structure of the nanoshells could be tuned by adjusting the molar ratio of monomers and silica particles. The nanoshells contained ~2.2 nm mesopores, facilitating the transport of drug molecules. They also exhibited excellent water dispersibility as well as biocompatibility; therefore, these nanoshells can be considered an ideal drug vehicle with high doxorubicin storage capacity (26.2 wt %) and excellent sustained released properties (up to 14 days). Interestingly, we found that the fluorescent PCTPF nanoshells not only delivered DOX into HeLa cells, but also killed them more effectively than DOX alone. Additionally, because of their fluorescence, the PCTPF nanoshells also provide a subtle mechanism for monitoring the release and distribution of DOX and its carriers.

■ ASSOCIATED CONTENT

Supporting Information

Size distribution of PCTPF nanoshells, TEM images of PCTPF nanoshells prepared at different mass ratios of SiO_2 to PCTPF precursors, photobleaching properties of fluorescein and PCTPF nanoshells, and pictures of fluorescein powder and PCTPF nanoshell powder under natural and 365 nm UV light. This material is available free of charge via the Internet at http://pubs.acs.org.

■ AUTHOR INFORMATION

Corresponding Authors

*E-mail: menglingjie@mail.xjtu.edu.cn.
*E-mail: qhlu@sjtu.edu.cn.

Author Contributions

#L.S. and T.L. contributed equally to this paper.

Notes

The authors declare no competing financial interest.

■ ACKNOWLEDGMENTS

This work was supported by National Science Foundation for Distinguished Young Scholars (50925310), the National Science Foundation of China (21174087, 21474079), the Major Project of Chinese National Programs for Fundamental Research and Development (973 Project: 2009CB930400), the Program for New Century Excellent Talents in University (NCET-13-0453), the China Postdoctoral Science Foundation (18420011, 2014T70909), and the Fundamental Funds for the Central Universities (08142027, 08143101). TEM and SEM measurements were also supported by the International Center for Dielectric Research at Xi'an Jiaotong University.

■ REFERENCES

(1) Hu, Y.; Jensen, J. O.; Zhang, W.; Cleemann, L. N.; Xing, W.; Bjerrum, N. J.; Li, Q. Hollow Spheres of Iron Carbide Nanoparticles Encased in Graphitic Layers as Oxygen Reduction Catalysts. *Angew. Chem., Int. Ed.* **2014**, *53*, 3675−3679.
(2) Yu, L.; Wu, H. B.; Lou, X. W. Mesoporous $Li_4Ti_5O_{12}$ Hollow Spheres with Enhanced Lithium Storage Capability. *Adv. Mater.* **2013**, *25*, 2296−2300.
(3) Zhang, W.-M.; Hu, J.-S.; Guo, Y.-G.; Zheng, S.-F.; Zhong, L.-S.; Song, W.-G.; Wan, L.-J. Tin-Nanoparticles Encapsulated in Elastic Hollow Carbon Spheres for High-Performance Anode Material in Lithium-Ion Batteries. *Adv. Mater.* **2008**, *20*, 1160−1164.
(4) Zhu, Y. F.; Shi, J. L.; Shen, W. H.; Dong, X. P.; Feng, J. W.; Ruan, M. L.; Li, Y. S. Stimuli-Responsive Controlled Drug Release from a Hollow Mesoporous Silica Sphere/Polyelectrolyte Multilayer Core-Shell Structure. *Angew. Chem., Int. Ed.* **2005**, *44*, 5083−5087.
(5) Caruso, F.; Caruso, R. A.; Mohwald, H. Nanoengineering of Inorganic and Hybrid Hollow Spheres by Colloidal Templating. *Science* **1998**, *282*, 1111−1114.
(6) Yang, M.; Cai, Q.; Liu, C.; Wu, R.; Sun, D.; Chen, Y.; Tang, Y.; Lu, T. Monodispersed Hollow Platinum Nanospheres: Facile Synthesis and Their Enhanced Electrocatalysis for Methanol Oxidation. *J. Mater. Chem. A* **2014**, *2*, 13738−13743.
(7) Xu, X. L.; Asher, S. A. Synthesis and Utilization of Monodisperse Hollow Polymeric Particles in Photonic Crystals. *J. Am. Chem. Soc.* **2004**, *126*, 7940−7945.
(8) Jin, Z.; Wang, F.; Wang, J.; Yu, J. C.; Wang, J. Metal Nanocrystal-Embedded Hollow Mesoporous TiO_2 and ZrO_2 Microspheres Prepared with Polystyrene Nanospheres as Carriers and Templates. *Adv. Funct. Mater.* **2013**, *23*, 2137−2144.
(9) Yu, J.; Guo, H.; Davis, S. A.; Mann, S. Fabrication of Hollow Inorganic Microspheres by Chemically Induced Self-Transformation. *Adv. Funct. Mater.* **2006**, *16*, 2035−2041.
(10) Shan, Z. W.; Adesso, G.; Cabot, A.; Sherburne, M. P.; Asif, S. A. S.; Warren, O. L.; Chrzan, D. C.; Minor, A. M.; Alivisatos, A. P. Ultrahigh Stress and Strain in Hierarchically Structured Hollow Nanoparticles. *Nat. Mater.* **2008**, *7*, 947−952.
(11) Park, J.; Zheng, H.; Jun, Y.-W.; Alivisatos, A. P. Hetero-Epitaxial Anion Exchange Yields Single-Crystalline Hollow Nanoparticles. *J. Am. Chem. Soc.* **2009**, *131*, 13943−13945.
(12) Yang, X.; Chen, Y.; Cao, Y.; An, L. Silicon Carbonitride Hollow Nanospheres from a Block-Copolymer Precursor. *J. Am. Ceram. Soc.* **2014**, *97*, 2387−2389.
(13) Niu, C.; Meng, J.; Han, C.; Zhao, K.; Yan, M.; Mai, L. VO_2 Nanowires Assembled into Hollow Microspheres for High-Rate and Long-Life Lithium Batteries. *Nano Lett.* **2014**, *14*, 2873−2878.
(14) Huang, J. X.; Xie, Y.; Li, B.; Liu, Y.; Qian, Y. T.; Zhang, S. Y. In-Situ Source-Template-Interface Reaction Route to Semiconductor CdS Submicrometer Hollow Spheres. *Adv. Mater.* **2000**, *12*, 808−811.
(15) Hu, P.; Yu, L.; Zuo, A.; Guo, C.; Yuan, F. Fabrication of Monodisperse Magnetite Hollow Spheres. *J. Phys. Chem. C* **2009**, *113*, 900−906.
(16) Guo, L.; Liang, F.; Wen, X.; Yang, S.; He, L.; Zheng, W.; Chen, C.; Zhong, Q. Uniform Magnetic Chains of Hollow Cobalt Mesospheres from One-Pot Synthesis and Their Assembly in Solution. *Adv. Funct. Mater.* **2007**, *17*, 425−430.
(17) Becker, M. L.; Remsen, E. E.; Wooley, K. L. Diblock Copolymers, Micelles, and Shell-Crosslinked Nanoparticles Containing Poly(4-fluorostyrene): Tools for Detailed Analyses of Nanostructured Materials. *J. Polym. Sci., Part A* **2001**, *39*, 4152−4166.
(18) Harrisson, S.; Wooley, K. L. Shell-Crosslinked Nanostructures from Amphiphilic AB and ABA Block Copolymers of Styrene-*alt*-(Maleic Anhydride) and Styrene: Polymerization, Assembly and Stabilization in One Pot. *Chem. Commun. (Cambridge, U.K.)* **2005**, 3259−3261.

DOI: 10.1021/acsami.5b00175
ACS Appl. Mater. Interfaces 2015, 7, 4990−4997

(19) Yang, T.-F.; Chen, C.-N.; Chen, M.-C.; Lai, C.-H.; Liang, H.-F.; Sung, H.-W. Shell-Crosslinked Pluronic L121 Micelles as a Drug Delivery Vehicle. *Biomaterials* **2007**, *28*, 725−734.
(20) Fang, Y.; Guo, S.; Li, D.; Zhu, C.; Ren, W.; Dong, S.; Wang, E. Easy Synthesis and Imaging Applications of Cross-Linked Green Fluorescent Hollow Carbon Nanoparticles. *ACS Nano* **2012**, *6*, 400−409.
(21) Wang, Z.; Wu, L.; Chen, M.; Zhou, S. Facile Synthesis of Superparamagnetic Fluorescent Fe_3O_4/ZnS Hollow Nanospheres. *J. Am. Chem. Soc.* **2009**, *131*, 11276−11279.
(22) Zhang, L. J.; Wang, M.; Wei, Y. Hollow Polyaniline Microspheres with Conductive and Fluorescent Function. *Macromol. Rapid Commun.* **2006**, *27*, 888−893.
(23) Tsou, C.-J.; Chu, C.-y.; Hung, Y.; Mou, C.-Y. A Broad Range Fluorescent Ph Sensor Based on Hollow Mesoporous Silica Nanoparticles, Utilising the Surface Curvature Effect. *J. Mater. Chem. B* **2013**, *1*, 5557−5563.
(24) Li, L.; Li, H.; Chen, D.; Liu, H.; Tang, F.; Zhang, Y.; Ren, J.; Li, Y. Preparation and Characterization of Quantum Dots Coated Magnetic Hollow Spheres for Magnetic Fluorescent Multimodal Imaging and Drug Delivery. *J. Nanosci. Nanotechnol.* **2009**, *9*, 2540−2545.
(25) Bottrill, M.; Green, M. Some Aspects of Quantum Dot Toxicity. *Chem. Commun. (Cambridge, U.K.)* **2011**, *47*, 7039−7050.
(26) Luo, J. D.; Xie, Z. L.; Lam, J. W. Y.; Cheng, L.; Chen, H. Y.; Qiu, C. F.; Kwok, H. S.; Zhan, X. W.; Liu, Y. Q.; Zhu, D. B.; et al. Aggregation-Induced Emission of 1-Methyl-1,2,3,4,5-pentaphenylsilole. *Chem. Commun. (Cambridge, U.K.)* **2001**, 1740−1741.
(27) Hong, Y.; Lam, J. W. Y.; Tang, B. Z. Aggregation-Induced Emission: Phenomenon, Mechanism and Applications. *Chem. Commun. (Cambridge, U.K.)* **2009**, 4332−4353.
(28) Hu, Y.; Meng, L.; Niu, L.; Lu, Q. Facile Synthesis of Superparamagnetic Fe_3O_4@Polyphosphazene@Au Shells for Magnetic Resonance Imaging and Photothermal Therapy. *ACS Appl. Mater. Interface* **2013**, *5*, 4586−4591.
(29) Hu, Y.; Meng, L.; Niu, L.; Lu, Q. Highly Cross-Linked and Biocompatible Polyphosphazene-Coated Superparamagnetic Fe_3O_4 Nanoparticles for Magnetic Resonance Imaging. *Langmuir* **2013**, *29*, 9156−9163.
(30) Zhou, J.; Meng, L.; Lu, Q. Core@Shell Nanostructures for Photothermal Conversion: Tunable Noble Metal Nanoshells on Cross-Linked Polymer Submicrospheres. *J. Mater. Chem.* **2010**, *20*, 5493−5498.
(31) Fu, J.; Chen, J.; Chen, Z.; Xu, Q.; Huang, X.; Tang, X. The Controlled Preparation of Cross-Linked Polyphosphazene Nanotubes of High Stability Via a Sacrificial Template Route. *New J. Chem.* **2010**, *34*, 599−602.
(32) Zhu, L.; Xu, Y.; Yuan, W.; Xi, J.; Huang, X.; Tang, X.; Zheng, S. One-Pot Synthesis of Poly(cyclotriphosphazene-*co*-4,4 '-sulfonyldiphenol) Nanotubes Via an in Situ Template Approach. *Adv. Mater.* **2006**, *18*, 2997−3001.
(33) Hu, Y.; Meng, L.; Lu, Q. "Fastening" Porphyrin in Highly Cross-Linked Polyphosphazene Hybrid Nanoparticles: Powerful Red Fluorescent Probe for Detecting Mercury Ion. *Langmuir* **2014**, *30*, 4458−4464.
(34) Joo, J. B.; Lee, I.; Dahl, M.; Moon, G. D.; Zaera, F.; Yin, Y. Controllable Synthesis of Mesoporous TiO_2 Hollow Shells: Toward an Efficient Photocatalyst. *Adv. Funct. Mater.* **2013**, *23*, 4246−4254.
(35) Liao, K.-H.; Lin, Y.-S.; Macosko, C. W.; Haynes, C. L. Cytotoxicity of Graphene Oxide and Graphene in Human Erythrocytes and Skin Fibroblasts. *ACS Appl. Mater. Interface* **2011**, *3*, 2607−2615.
(36) Sato, T.; Horiuchi, T.; Nishimura, I. Simple and Rapid Determination of Histamine in Food Using a New Histamine Dehydrogenase from *Rhizobium* sp. *Anal. Biochem.* **2005**, *346*, 320−326.
(37) Huang, X.; Wei, W.; Zhao, X.; Tang, X. Novel Preparation of Polyphosphazene-Coated Carbon Nanotubes as a Pt Catalyst Support. *Chem. Commun. (Cambridge, U.K.)* **2010**, *46*, 8848−8850.
(38) Wang, L. L.; Roitberg, A.; Meuse, C.; Gaigalas, A. K. Raman and FTIR Spectroscopies of Fluorescein in Solutions. *Spectrochim. Acta, Part A* **2001**, *57*, 1781−1791.
(39) Breza, M. The Electronic Structure of Planar Phosphazene Rings. *Polyhedron* **2000**, *19*, 389−397.
(40) Liu, Z.; Fan, A. C.; Rakhra, K.; Sherlock, S.; Goodwin, A.; Chen, X.; Yang, Q.; Felsher, D. W.; Dai, H. Supramolecular Stacking of Doxorubicin on Carbon Nanotubes for in Vivo Cancer Therapy. *Angew. Chem., Int. Ed.* **2009**, *48*, 7668−7672.
(41) Borges, O.; Cordeiro-da-Silva, A.; Romeijn, S. G.; Amidi, M.; de Sousa, A.; Borchard, G.; Junginger, H. E. Uptake Studies in Rat Peyer's Patches, Cytotoxicity and Release Studies of Alginate Coated Chitosan Nanoparticles for Mucosal Vaccination. *J. Controlled Release* **2006**, *114*, 348−358.
(42) Arcos, D.; Lopez-Noriega, A.; Ruiz-Hernandez, E.; Terasaki, O.; Vallet-Regi, M. Ordered Mesoporous Microspheres for Bone Grafting and Drug Delivery. *Chem. Mater.* **2009**, *21*, 1000−1009.
(43) Cunningham, C. L.; Martinez-Cerdeno, V.; Noctor, S. C. Microglia Regulate the Number of Neural Precursor Cells in the Developing Cerebral Cortex. *J. Neurosci.* **2013**, *33*, 4216−4233.
(44) Markaki, Y.; Smeets, D.; Fiedler, S.; Schmid, V. J.; Schermelleh, L.; Cremer, T.; Cremer, M. The Potential of 3D-FISH and Super-Resolution Structured Illumination Microscopy for Studies of 3D Nuclear Architecture. *Bioessays* **2012**, *34*, 412−426.

DOI: 10.1021/acsami.5b00175
ACS Appl. Mater. Interfaces 2015, 7, 4990−4997